Separation Science and Technology
Publication details, including instructions for authors and subscription information:
http://www.informaworld.com/smpp/title~content=t713708471

Concentration and Analysis of Dilute Colloidal Samples by Sedimentation Field-Flow Fractionation

J. C. Giddings[a]; G. Karaiskakis[a]; K. D. Caldwell[a]
[a] DEPARTMENT OF CHEMISTRY, UNIVERSITY OF UTAH SALT LAKE CITY, UTAH

To cite this Article Giddings, J. C. , Karaiskakis, G. and Caldwell, K. D.(1981) 'Concentration and Analysis of Dilute Colloidal Samples by Sedimentation Field-Flow Fractionation', Separation Science and Technology, 16: 6, 725 — 744
To link to this Article: DOI: 10.1080/01496398108058124
URL: http://dx.doi.org/10.1080/01496398108058124

SEPARATION SCIENCE AND TECHNOLOGY, 16(6), pp. 725-744, 1981

Concentration and Analysis of Dilute Colloidal Samples by Sedimentation Field-Flow Fractionation

J. C. GIDDINGS, G. KARAISKAKIS, and K. D. CALDWELL

DEPARTMENT OF CHEMISTRY
UNIVERSITY OF UTAH
SALT LAKE CITY, UTAH 84112

ABSTRACT

An on-channel concentration procedure is described in which large volumes of dilute colloidal materials can be concentrated at the head of an FFF channel in preparation for separation and analysis. The theory of the procedure is described, with particular focus on expected perturbations in retention and plate height due to the finite initial zone length. Two sizes (0.357 and 0.481 μ m) of polystyrene latex beads diluted in volumes of up to 50 ml are used as model colloids. Separation of the two bead sizes is demonstrated. The beads are then subjected to careful retention and plate height measurements and the results compared to theoretical expectations. Certain anomalies are noted which may relate to the reversible adhesion of the particles to the channel wall. Possible extensions and ramifications of the technique are noted.

INTRODUCTION

Sedimentation field-flow fractionation is the FFF subtechnique which utilizes a centrifugal or gravitational field to sediment component particles into the characteristic steady-state layer against the channel wall. The thickness of the layer is an explicit function of the applied field, particle size, and the

density of both the particles and the carrier solution. The largest particles, of course, are forced most vigorously toward the channel wall where flow velocity is lowest and, therefore, these particles become the most highly retained. The fractogram (a graph of detector response versus the volume of carrier solution eluted) becomes a linear mass spectrum for well retained particles (1).

Sedimentation FFF shows remarkable resolution in the separation of colloidal size particles (2). The characterization of these particles proceeds from two types of observations: 1) retention volume V_r is specifically dependent on particle size and density, and 2) plate height (measuring zone spreading or peak width) is a function of the diffusion rate and polydispersity of the sample. A number of different materials (including viruses, latices, and emulsions) have been characterized using the conventional sample injection technique (3). In this case, a few microliters of a fairly concentrated sample (of the order of 1 to 10% solids) are injected onto the head of the channel while the carrier solution is flowing. The flow is then stopped and the field applied by starting the rotation of the centrifuge. After an appropriate stop-flow time in which the sample relaxes into its characteristic steady-state layer thickness, the flow is started and the fractogram is generated.

In this paper, a technique for dealing with large (up to 50 ml) volumes of dilute colloidal materials is presented. The process consists of two steps. In the concentration step, the sample is pumped into the rotating centrifuge under conditions of low flow and high field and is thereby concentrated at the head of the channel. In the separation step, the field strength is lowered and the flow rate increased in order to obtain the normal migration and elution of the sample. The flow rate and field strength can be optimized independently in the two steps.

Kirkland et al. have also proposed the use of high initial field strengths to concentrate samples in sedimentation (FFF) (4). Their work does not include the concept of changing flow

rate as well as field strength to optimize the overall procedure.

In order to test the validity of this procedure of on-channel concentration, a series of fractograms of well characterized monodisperse latices were run in which the amount of the sample was held constant while the volume in which it was contained was varied over a 50,000-fold range. Retention and zone spreading showed a surprisingly small effect in spite of the large sample volume injected. This makes sedimentation FFF a highly attractive technique for the characterization of samples (such as those of natural water) where particles are present in low concentration.

THEORY

The underlying theory of the present technique divides into two parts: the basic theory applicable to normal FFF operation, which extends as well to the on-column concentration technique, and the theory peculiar to on-column concentration. We will also discuss in this section the ways in which theory can be used for sample characterization.

Basic Theory.

In FFF, the application of a field results in the formation of an exponential steady-state layer in which particle concentration c varies with distance x from the wall as (5)

$$c = c_o \exp(-x/\ell) \qquad (1)$$

where c_o is the concentration at the wall and ℓ is a characteristic layer dimension termed the mean layer thickness. The dimensionless retention parameter λ is related to ℓ by

$$\lambda = \ell/w \qquad (2)$$

where w is the channel thickness.

In FFF, as in chromatography, the degree of retention can be measured by the retention ratio R, which is the ratio of the velocity of the retained component to that of a void (nonretained) peak. Parameter R is a function only of λ

$$R = 6\lambda[\coth(1/2\lambda) - 2\lambda] \quad (3)$$

As λ approaches zero (well retained components), the above relationship can be simplified to

$$R = 6\lambda \quad (4)$$

The retention parameter λ is determined by experimental parameters and physical constants as follows

$$\lambda = D/Uw = R'T/Fw \quad (5)$$

where D is the particle diffusion coefficient, U is the mean lateral drift velocity induced by the field which exerts force F, R' is the gas constant, and T is the absolute temperature.

For sedimentation FFF applied to spherical particles, Equation 5 becomes (6)

$$\lambda = 6kT/\pi d^3 Gw\Delta\rho \quad (6)$$

where k is Boltzman's constant, G is the angular acceleration ($\omega^2 r$, ω being the angular velocity) about radius r, d is the diameter of the particle, and $\Delta\rho$ is the difference between the density of the particle and that of the carrier solution.

The above considerations apply to the downstream migration of particles under steady-state conditions. However, there is an important transient period τ in which the particles relax into the steady-state configuration. Quantity τ is approximated by the ratio of the maximum relaxation distance a particle must travel,

equal to channel thickness w, divided by the field-induced velocity U

$$\tau = w/U \tag{7}$$

If we use $U = D/w\lambda$, obtained from Equation 5, in this expression, we get

$$\tau = w^2\lambda/D \tag{8}$$

We now use the Stokes-Einstein equation for D

$$D = kT/3\pi\eta d \tag{9}$$

and Equation 6 for λ, thus transforming Equation 8 to

$$\tau = 18\eta w/G\Delta\rho d^2 \tag{10}$$

When using the stop-flow method, flow should be halted for this period of time as calculated for the smallest retained particles in the sample. Since the stop-flow method cannot be used for the continuous injection procedure employed here, the effect of relaxation on sample behavior must be evaluated.

This will be done in the next subsection. We turn now to zone broadening, which affects the resolution obtainable in attempting to separate and analyze particles of different size. Zone broadening in FFF can be accounted for by the following plate height Equation (5)

$$H = 2D/R\langle v\rangle + \chi w^2\langle v\rangle/D + \Sigma H_i \tag{11}$$

where the first term accounts for molecular diffusion along the channel axis (usually negligible in sedimentation FFF), the second is a nonequilibrium or mass transfer term, and the third consists

of contributions due to nonideal processes in the system and the sample. The mean carrier velocity <v> is an important parameter from an experimental viewpoint because it can be varied readily and can be used to sort out the terms of Equation 11.

The nonequilibrium coefficient χ is a complex function of λ which assumes the value

$$\chi = 1/105 \tag{12}$$

for the limit of no retention (R = 1) and

$$\chi = 24\lambda^3 \tag{13}$$

for high retention ($R,\lambda \to 0$).

The third term of Equation 11 has been found to derive almost entirely from a sample polydispersity contribution H_p under ideal experimental conditions, in which a small concentrated sample is injected directly on the column (7). However, with the on-column concentration procedure, some new terms contribute to ΣH_i. These must be evaluated to establish conditions which assure us that high resolution will be maintained.

On-Column Concentration Theory.

The continuous injection of large volumes of sample effectively introduces a sample slug of finite length at the head of the channel, before the separation step begins. The finite sample slug has the effect of increasing plate height and interfering with resolution because of its length, and, to some degree, reducing retention volumes because the center of gravity of the sample is advanced further into the channel before separation commences.

Two processes contribute to the formation and finite length of the sample slug. First, as a small volume element of sample enters the channel and distributes over its cross section, relaxa-

tion commences but affects differently particles in different parts of the cross section. Particles next to the outside (or accumulation) wall are held there and do not migrate any significant distance during relaxation time τ. Particles at the inside (or evacuation) wall are swept downstream at mean velocity $\langle v_f \rangle$ as they traverse the channel, thus migrating a distance

$$h_o = \langle v_f \rangle / \tau \tag{14}$$

during relaxation time τ (8). Particles starting at other points of the cross section end up somewhere between zero and h_o downstream. The overall distribution of particles over distance h_o is bimodal (8).

A second process contributing to the finite length of the sample slug is the continuous (but slow) FFF migration of the initial part of the deposited slug during the period in which the latter part is being fed into the channel. Over the duration of the concentration or feed step t_f, a sample with retention ratio R_f will distribute itself along a fraction of the channel length equal to $R_f V_f / V^o$, where V_f is the feed volume of the introduced sample and V^o is the channel void volume. Since the fraction of the total channel length L occupied by sample is the above ratio $R_f V_f / V^o$, the length of occupancy s_o is

$$s_o = R_f V_f L / V^o \tag{15}$$

The combined effect of sample relaxation and sample migration during the concentration step leads to the positioning of the center of gravity of the sample slug at a distance of approximately

$$Z_{cg} = (h_o + s_o)/2 \tag{16}$$

from the head of the channel. The center of gravity of the eluted peak will thus emerge earlier than expected according to the time

ratio $(L-Z_{cg})/L$. Thus the apparent R value, R_{app}, measured by means of elution time or volume, will be higher than the true value by the ratio

$$\frac{R_{app}}{R_{true}} = \frac{L}{L - Z_{cg}} = \frac{L}{L-(h_o + s_o)/2} \qquad (17)$$

If this ratio differs significantly from unity, the observed R should be corrected to its true value. However, this may be difficult to do exactly for real world samples (for example, nonspherical particles) because of the difficulty of calculating τ exactly and the problem of estimating R_f under the high field conditions of the concentration step in which complicated steric and wall adhesion effects might affect migration.

Another concern is the effect of finite slug length on zone broadening as measured by plate height. To a good approximation we can assume that the relaxation and the migration contributions to plate height are independent and additive. Thus the extra plate height term in Equation 11, ΣH_i, consists of the three terms

$$\Sigma H_i = H_p + H_f = H_p + H_r + H_m \qquad (18)$$

where H_p is the sample polydispersity contribution mentioned earlier and H_f is the total feed contribution consisting of the relaxation contribution H_r and the migration component H_m.

It has been shown that the relaxation contribution amounts to (8,9)

$$H_r = 17h_o^2/140L \qquad (19)$$

Migration, on the other hand, has the effect of starting the sample out as a uniform slug distributed over distance s_o. This yields a plate height contribution of (10)

$$H_m = s_o^2/12L \qquad (20)$$

Thus the total feed contribution--the part unique to the on-column concentration method--is given by

$$H_f = H_r + H_m = \frac{17h_o^2}{140L} + \frac{s_o^2}{12L} \qquad (21)$$

We have ignored here as a second order effect the perturbation of Equation 11 by the fact that the zone is not generating its calculated plate height values over its entire length. The zone is instead subject to one plate height value for any migration occurring in the concentration step and another for migration during the separation step, for which the mean migration path length is L - Z_{cg} rather than L.

Several criteria can be developed to make sure that H_f is not excessive. It is possible, for example, to require that H_f not exceed a certain fraction of the total plate height. However, since the other components of plate height vary widely according to experimental and sample conditions, it is perhaps best to establish some reasonable performance ceiling to which we are confined by virtue of H_f. Most simply, we can require that H_f confine us to no fewer than N_f theoretical plates

$$N_f = \frac{L}{H_f} = \frac{4L^2}{17h_o^2/35 + s_o^2/3} \qquad (22)$$

For example, if h_o is negligible, a ten percent occupancy by the initial sample slug, $s_o/L = 0.1$, will permit $N_f = 1200$ plates, while a twenty percent occupancy will establish a ceiling of N_f = 300 plates. If both $s_o/L = 0.1$ and $h_o/L = 0.1$, $N_f = 488$ plates. The other plate height processes will reduce the plate count below N_f. However, a few hundred plates are sufficient for exceptional mass resolution in sedimentation FFF because of the high selectivity of the latter. For example, 400 total plates are sufficient to resolve (at unit resolution) particles differing in mass by only 20 percent, which for spheres corresponds to a diameter difference of only 6.2 percent (11).

The above arguments suggest that for most particle analysis, the initial slug is adequately narrow if its two contributing parts occupy no more than ten percent of the channel each: $h_o/L \leq 0.1$, $s_o/L \leq 0.1$. In order to realize the first condition it is advantageous to impose high fields and limited flow during the concentration step using a channel of narrow width. The second condition is most easily realized using high fields (unless the steric transition is exceeded) and limited sample dilution. It might be possible to further limit s_o by grooving, roughening, or depositing a thin porous layer on the first ten or so percent of the accumulation wall to retard FFF migration in the concentration step provided migration in the separation step was not adversely affected. Parameter s_o might be reduced also by establishing conditions conducive to reversible adhesion, which phenomenon appears to be occurring in the present system (see below).

Sample Characterization.

We have developed methods for extracting accurate information on mean particle diameter (or volume for nonspherical particles), standard deviation in diameter or volume, and particle density using small concentrated samples. These methods can be extended to dilute samples like those used here with certain precautions. Our characterization work has so far dealt with samples of low polydispersity but could be extended to high polydispersity samples (continuous distribution) dealing individually with narrow cuts from a broad spectrum fractogram.

We note first of all that λ is uniquely related to particle diameter d through Equation 6 and that R depends on λ as shown in Equation 3. Thus it is possible in favorable circumstances to derive mean d values to within about one percent accuracy using FFF retention (7). The equation can be very simply extended to particle volume for nonspherical particles. The method is applicable to dilute samples using on-column concentration provided the ratio in Equation 17 is within a few percent of unity or that a correction is made for the departure from unity.

It is also possible to measure particle density by measuring retention in carriers of two or more different densities.

Equation 11 suggests that a plot of plate height H vs flow velocity $\langle v \rangle$ is a straight line (since the first term is negligible at all practical velocities) whose slope yields the ratio χ/D. Both χ and D relate to particle diameter d (see Equations 13 and 6 along with Equation 9), and can be used to confirm the value of d obtained from retention measurements. Alternately, D can be used independently to determine d, and the λ from retention measurements can be used to determine $\Delta\rho$, thus yielding the density for spherical particles whose density is not known. For nonspherical particles, D can be used independently to characterize particle shape.

The intercept of the H versus $\langle v \rangle$ curve should equal the sum of H_p and H_f in Equation 18. If H_f is negligible or can be calculated, H_p can be obtained from the intercept and can be used to characterize sample polydispersity (7).

EXPERIMENTAL

Apparatus and Materials.

A standard model of the sedimentation FFF apparatus described previously (3) was used in these studies. The channel dimensions were: length L = 83.3 cm, width w = 0.0254 cm, and breadth a = 2.0 cm. The void volume of this channel was measured as 4.5 ml by elution of a nonretained peak. The channel was positioned 7.7 cm from the center of rotation. A Gilson Minipuls 2 peristaltic pump was used to feed the sample during the concentraton step and to maintain flow during the separation step. A Beckman UV Monitor (Model 153) was used for detection at 254 nm. An Omniscribe strip chart recorder (Houston Instruments) was used to record the fractograms.

The samples were monodisperse polystyrene latex beads (Dow Chemical Co.) with nominal diameters of 0.357 ± 0.0056 μm and

0.481 ± 0.0018 μm. These were obtained from the manufacturer as dispersions containing 10% solids. They were either used in that form or diluted with the carrier solution to study sample dilution effects. The carrier was doubly distilled water containing 0.1% by volume Fl-70 detergent (Fisher Scientific Co.) and 0.02% by weight sodium azide as a bacteriocide. The carrier solution was degassed prior to use by heating to 70°C.

Experimental Procedure.

1. 0.357 μm Beads. Diluted samples were prepared by adding 1 μl of the 10% solids sample to 1, 5, 10, 20, 30, 40, and 50 ml of carrier solution. Standard fractograms were run with 1 μl of the undiluted 10% solids sample using the normal procedure of injecting the sample onto the column with a microsyringe, stopping the flow to relax the sample for 4.41 minutes at 1800 rpm, then reducing the field to 880 rpm to elute the sample at flow rates ranging from 12.6 to 52.5 ml/hr. A series of fractograms with diluted samples was then obtained where the concentration step consisted of pumping the diluted sample at a rate of 5.80 ml/hr into the channel while it was rotating at 1800 rpm. When the sample was consumed, pumping was continued at the same rate with 3.4 ml of carrier solution to clear the sample from the pump. Then the field was reduced and flow rate increased to elute the sample. The relaxation time under these conditions was calculated to be 4.41 minutes. Retention volumes V_r and plate heights H were measured for each fractogram.

2. 0.481 μm Beads. Diluted samples were prepared by adding 1 μl of 10% solids sample to 5, 10, 20, and 50 ml of carrier solution. The experimental procedure above was repeated except that the conditions during sample feed were a flow rate of 7.58 ml/hr and a field of 1400 rpm. Elution was at 500 rpm at flow rates ranging from 24.1 to 53.9 ml/hr. Relaxation time for this particle under these conditions was 3.35 minutes.

RESULTS AND DISCUSSION

Figure 1 provides a comparison of fractograms for the 0.357 μm beads injected as a narrow pulse (top) and injected at 10 ml dilution (bottom) by the procedure described here. The figure shows that the eluted peak from the diluted sample emerges intact and without serious degradation despite the fact that the sample volume (10 ml) is over twice the channel volume (4.5 ml).

Table 1 lists the apparent retention ratio R_{app} as measured for both of the particle standards at the dilutions given. Also

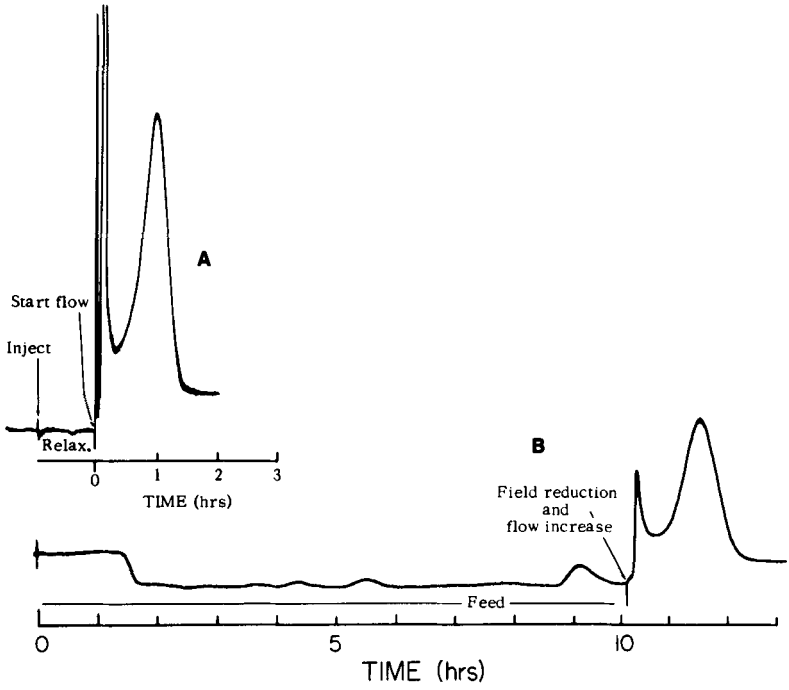

FIGURE 1. Retention of polystyrene latex beads of 0.357μ m diameter following A direct injection of 1 μl sample and B feed-injection of 10 ml sample. The amount of solids was 0.1 mg in both cases, and the working field was 880 rpm. In case B, the concentation step was carried out while pumping at 5.8 ml/h with the channel spinning at 1800 rpm. In the separation step, the flow rates were 35.2 ml/h (A) and 30.8 ml/h (B).

TABLE 1

Retention Ratio and other Parameters for 0.1 mg Samples of Two Polystyrene Latex Beads of Nominal Diameters 0.357 μm and 0.481 μm Diluted in Feed Volume V_f.

V_f (ml)	$R_{app}=V^o/V_r$ (exp)	h_o/L (theor)	s_o/L (theor)	R_{app}/R_{true} (theor)	R_{app} (theor)
		Bead Diameter (μm): 0.357			
0	-	0.0	0.0	1.0	0.120
1	0.122	0.100	0.007	1.056	0.127
5	0.124	0.100	0.035	1.072	0.129
10	0.124	0.100	0.071	1.093	0.131
20	0.124	0.100	0.141	1.137	0.136
30	0.124	0.100	0.212	1.185	0.142
40	0.124	0.100	0.283	1.237	0.148
50	0.124	0.100	0.353	1.293	0.155
		Bead Diameter (μm): 0.481			
0	-	0.0	0.0	1.0	0.118
5	0.123	0.100	0.019	1.063	0.125
10	0.119	0.100	0.037	1.074	0.127
20	0.120	0.100	0.074	1.095	0.129
14	0.121	0.100	0.185	1.166	0.138

shown are the ratios h_o/L and s_o/L, calculated by means of Equations 14 and 15, respectively. The top row of the table for each of the particle diameters shows only the theoretical entries for R_{app} (0.120 and 0.118) calculated by means of Equations 6 and 3. This calculation is based on a delta function starting zone, $h_o = s_o = 0$. We consider this value quite reliable based on our earlier observations of a close correspondence between theory and experiment (7).

According to Equation 17, the measured retention ratios R_{app} shown in the table should increase significantly with increasing feed volume because of the concurrently increasing s_o value. The magnitude of the theoretically expected increase is shown in the last column. However, beyond a small overall increase in R_{app} with respect to the base values of 0.120 and 0.118 for the two beads, there is essentially no trend with increasing V_f. This failure to follow the theoretical trend appears to relate to recent observations in our laboratory that colloidal particles often adhere to the column wall at high fields, but are released when field strength is reduced to some more or less discrete value. We thus suggest that our results are consistent with the concept that the relaxation contribution (expressed through h_o) occurs much as expected but that the particles adhere to the wall soon after contact, thus reducing s_o essentially to zero.

Support for this mechanism was found when we attempted to separate the two particle standards (d_p = 0.357 and 0.481 μm) initially mixed together in a volume V_f of 10 ml. The mixture was fed into the channel at a rate of 5.8 ml/hr while the channel was rotating at 1800 rpm; the field was subsequently reduced to a working level of 880 rpm for the separation step. This working field was expected to cause elution of the smaller beads at 34 ml and the larger beads at 114 ml. The smaller beads did elute at 34 ml as predicted, but the larger particles had still not appeared after 150 ml. A reduction in the field to 300 rpm immediately released the heavier beads. Figure 2 demonstrates this type of stepwise field reduction. Despite the anomalous retention, the two particle sizes are almost baseline resolved. Thus, while as yet poorly understood, the wall adhesion is not necessarily detrimental to separation since field programming can readily be used to release the immobilized zones. Also, if wall adhesion truly reduces s_o to a value near zero, the potential feed volume will be even higher than expected and the perturbation to retention and plate height less significant than calculated.

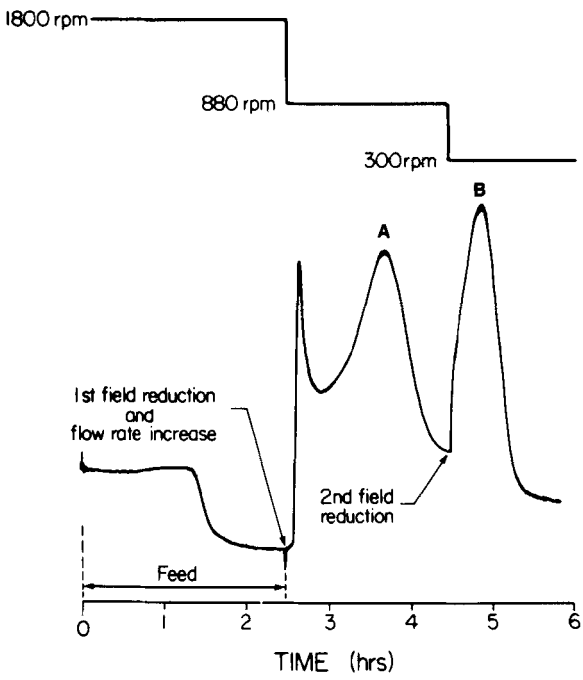

FIGURE 2. Separation of a dilute mixture of two types of latex spheres with nominal diameters 0.357 μm (A) and 0.481 μm (B). The sample volume (10 ml) was fed to the spinning channel (1800 rpm) at a rate of 5.8 ml/h. The working flow rate was 30.5 ml/h; the working field was reduced from 880 rpm to 300 rpm immediately following elution of the 0.357 μm beads.

Plate height data were also accumulated in order to examine the effect of sample dilution and other parameters on zone broadening and thus on resolution. Most instructive are plots of H versus the mean working velocity <v>. These plots are shown in Figure 3 for the 0.357 μm beads at different dilutions. The data tend to fall on a straight line of positive slope, as predicted on the basis of Equation 11. Clearly, the plate height increases with sample dilution but the slope remains nearly unchanged, all in accord with theory.

The H vs <v> results for all experimental cases were subjected to linear regression, yielding the intercept and slope values

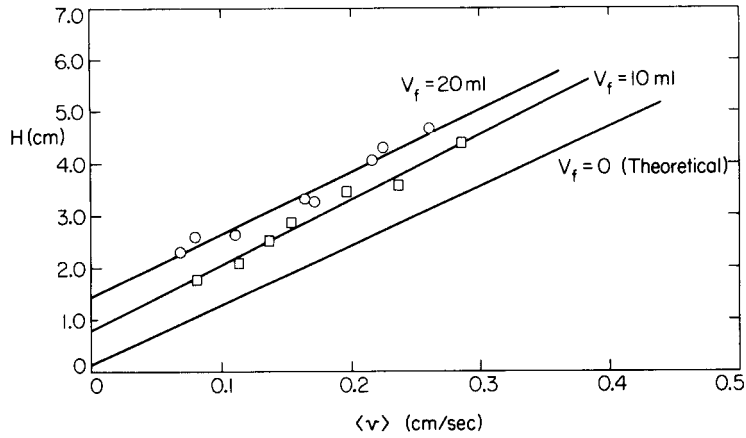

FIGURE 3. Plate height H versus working flow velocity ⟨v⟩ for 0.357 μm latex beads diluted in volume V_f. The concentration or feed step proceeded at $\langle v_f \rangle$ = 5.76 ml/h at 1800 rpm. The rotation rate was reduced to 880 rpm for separation/elution.

shown in Table 2. The slopes obtained in this way are in good agreement with the theoretical values, especially for the 0.357 μm beads. However, the intercepts show a large discrepancy, with the experimental values systematically larger. The reasons for the discrepancy are unclear. If the particles adhere reversibly to the wall as suggested by the retention studies, the experimental results should be reduced, not increased, with respect to the theoretical values. Perhaps the adsorption and desorption steps are both slow, causing additional zone dispersion which would appear in the intercept term. More study is needed regarding these phenomena.

CONCLUSIONS

The results of this study show that the on-column concentration method works quite successfully in dealing with highly diluted samples. Optimization, particularly higher field strengths during the concentration step, would allow higher flow rates and

TABLE 2

Results of Plate Height versus Velocity Studies for Polystyrene Latex bead Samples at Various Diluted Volumes V_f. Experimental Conditions in Text.

V_f	Slope(seconds)		Intercept (cm)				
(ml)	$dH/d\langle v\rangle$ (theor)	$dH/d\langle v\rangle$ (exp)	H_p (theor)	H_r (theor)	H_m (theor)	ΣH_i (theor)	H (exp)
			Bead Diameter (μm): 0.357				
10^{-3}	11.38	11.93	0.15	0	0	0.15	0.25
10	11.38	12.64	0.15	0.10	0.03	0.28	0.78
20	11.38	11.94	0.15	0.10	0.14	0.39	1.44
			Bead Diameter (μm): 0.481				
10^{-3}	15.73	14.26	0.01	0	0	0.01	0.30
10	15.73	13.41	0.01	0.10	0.01	0.12	0.56
20	15.73	12.66	0.01	0.10	0.04	0.15	0.62
50	15.73	13.03	0.01	0.10	0.24	0.35	0.67

increased analysis speed. However, experimental confirmation would be necessary to give assurance that the particle-wall adhesion did not become irreversible at higher spin rates. For samples of natural particulate systems, possible differences in adhesion characteristics for different types of particles would have to be accounted for.

Clearly, by extrapolation, the present methodology for dilute samples would work for other FFF subtechniques such as flow FFF, thermal FFF and electrical FFF. It would work well in conjunction with programmed systems since programmed runs begin at high field strengths as a matter of course (12). The methodology would couple effectively with the Kirkland-Yau exponential programming with delay (13), except that the theoretical interpretation would

be complicated if different flow velocities were used in the concentration and separation steps.

Theoretically, the results of the present study are puzzling in several respects, particularly the unexpected constancy of R_{app} and the excessively large plate height intercepts. However, with care, it should still be possible to do accurate particle characterization work. The constancy of R_{app} makes it especially simple to measure particle size for single cuts or particle size distributions for the entire sample. Density parameters should be measurable as before by varying the density of the carrier. Since the experimental and theoretical slopes of the plate height plots are in good agreement, the slopes can be used to obtain diffusivity or density data, as suggested in the theoretical section. However, the poor agreement of intercepts means that polydispersity values for narrow fractions would presently be difficult to measure.

ACKNOWLEDGMENT

This work was supported by Department of Energy Grant DEC02-79 EV10244A000.

REFERENCES

1. J. C. Giddings, M. N. Myers, F. J. Yang, and L. K. Smith, in Colloid and Interface Science, Vol. IV, M. Kerker, ed., Academic press, New York, 1976.

2. J. C. Giddings, K. D. Caldwell, J. F. Moellmer, T. H. Dickinson, M. N. Myers, and M. Martin, Anal. Chem. 51, 30 (1979).

3. J. C. Giddings, M. N. Myers, K. D. Caldwell, S. R. Fisher, in Methods of Biochemical Analysis, D. Glick, ed., John Wiley, New York, 1980, p. 79.

4. J. J. Kirkland, W. W. Yau, W. A. Doerner, and J. W. Grant, Anal. Chem. 52, 1944 (1980).

5. E. Grushka, K. D. Caldwell, M. N. Myers, and J. C. Giddings, Separation and Purification Methods 2, 127 (1973)

6. J. C. Giddings, F. J. F. Yang, and M. N. Myers, and J. C. Giddings, Anal. Chem. 46, 1917 (1974).
7. G. Karaiskakis, M. N. Myers, K. D. Caldwell, and J. C. Giddings, Anal. Chem. 53, 000 (1981).

8. M. E. Hovingh, G. H. Thompson, and J. C. Giddings, Anal. Chem., 42, 195 (1970).

9. F. J. Yang, M. N. Myers, and J. C. Giddings, Anal. Chem. 49, 659 (1977).

10. J. C. Giddings, Dynamics of Chromatography. Part I., Marcel Dekker, New York, 1965, p. 90.

11. J. C. Giddings, Pure & Appl. Chem. 51, 1459 (1979).

12. F. J. F. Yang, M. N. Myers, and J. C. Giddings, Anal. Chem. 46, 1924 (1974).

13. W. W. Yau and J. J. Kirkland, Sep. Sci. and Technol. 16, 000 (1981).